Organic & Biomolecular Chemistry

Accepted Manuscript

This article can be cited before page numbers have been issued, to do this please use: E. R. Morton, M. J. Porter, J. R. Baker, V. Chudasama and C. J. E. Haynes, *Org. Biomol. Chem.*, 2025, DOI: 10.1039/D5OB01392E.

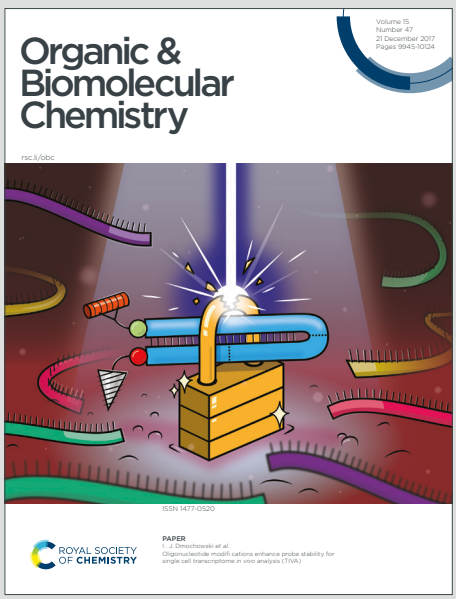

ROYAL SOCIETY OF CHEMISTRY

rsc.li/obc

View Article Online
DOI: 10.1039/D5OB01392E

ARTICLE

Bis-amino maleimides: a new class of dual hydrogen bond donor for anion binding and transport

Evelyn R. Morton, Michael J. Porter, James R. Baker, Vijay Chudasama and Cally J. E. Haynes*

Received 00th January 20xx,
Accepted 00th January 20xx

DOI: 10.1039/x0xx00000x

Dual hydrogen bond donor scaffolds are used in the design of numerous supramolecular receptors and play an important role in the specific recognition, reaction and transport of anionic guests. In this work, we detail the synthesis of symmetrical and unsymmetrical bis-amino maleimides as dual hydrogen bond donors and report their anion recognition and transport properties. DFT studies provide insight into the conformational preferences and binding properties of these receptors. Compared to existing dual hydrogen bond donors, the bis-amino maleimide motif contains an additional handle for synthetic functionalisation and thus offers the opportunity to tune the substituent properties to fit a desired function.

Introduction

The design of synthetic receptors for the supramolecular recognition of anions is important for a range of applications in biology, medicine, and environmental remediation. [1-4] Using receptors as anionophores – to transport ions across cell membranes – is one such application, with potential utility in combating channelopathies like cystic fibrosis which results from faulty chloride transport across the cell membrane, as well as novel treatments for cancer and microbial infections. [5-19] In recent years, there has been a concerted effort to design and develop biocompatible anionophores to act as therapeutics with the key properties of lipophilicity, highly selective and strong complexation to the anion of interest, and non-toxicity. [20-23] Hydrogen bonding is arguably the most commonly utilised approach to anion recognition, leading to the development of a class of molecules termed 'dual hydrogen bond donors' containing two convergent hydrogen bond donors that can effectively chelate an anion. (Thio)ureas[24, 25] and members of the cyclic oxocarbon family, including squaramides, [20, 26-29] deltamides and croconamides, [30, 31] have proved extremely effective in selective anion recognition. In 2023, Costa and co-workers reported that photochemically transforming squaramide anion transporters into bis-amino maleic anhydrides effectively switched off their transport activity. [32] A common characteristic of these established motifs is that they each contain two substituents (R groups – **Figure 1**) for synthetic diversification, which offers the potential to fine-tune the binding strength (e.g. through electronic considerations) solubility/ lipophilicity[33] and mobility, [34] as well as opportunities to append a broad array of functional units

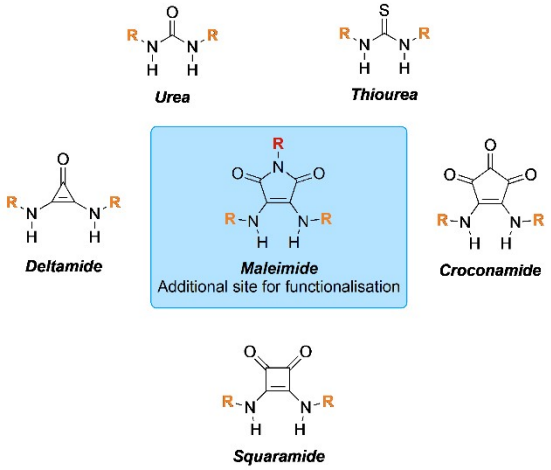

Figure 1 Structures of existing dual hydrogen bond donors alongside the potential maleimide scaffold. R groups denote positions for potential synthetic functionalisation.

such as fluorophores, [35] organelle targeting groups, [36] chiral groups, [37] stimuli-responsive groups[13, 14, 38-42] and tethers to solid supports. [43, 44] Increasing the opportunity for the synthetic diversification of functional anion receptors is therefore a valuable target.

The maleimide motif is an important building block in organic synthesis and its use in peptide and protein bioconjugation has been widely reported. [45-47] However, to our knowledge bis-amino maleimides have not previously been investigated as dual hydrogen bond donor receptors. We hypothesised that the rigid five-membered electron-deficient ring structure of the maleimide core, combined with two projecting hydrogen bond donors could make these molecules a promising scaffold for anion recognition and transport. Compared to the other scaffolds in **Figure 1**, they offer an additional synthetic handle on the imide nitrogen, allowing for further diversification and

Department of Chemistry, University College London, 20 Gordon Street, London WC1H 0AJ, UK. Email: cally.haynes@ucl.ac.uk

View Article Online
DOI: 10.1039/D5OB01709E

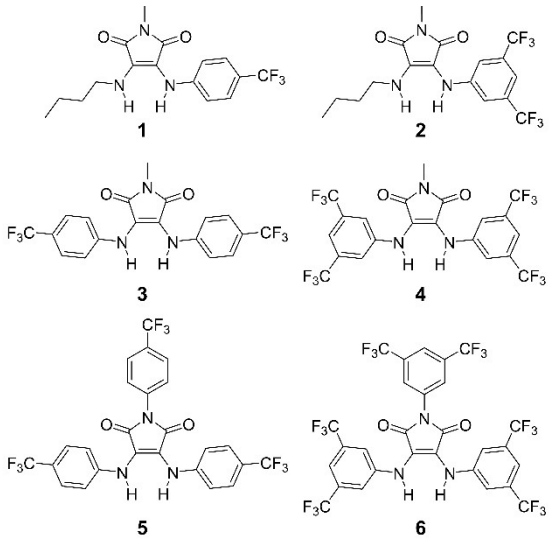

Figure 2 Library of unsymmetrical and symmetrical bis-amino maleimides (**1**–**6**).

for the electron density of the ring to be tuned. In this report, we discuss the synthesis, anion recognition and anion transport properties of six novel symmetrical and unsymmetrical bis-amino maleimides (**1**–**6**, **Figure 2**) to study the impact of the additional synthetic handle on their ability to function as anion receptors and transporters.

Design and synthesis

We conceived that the series of bis-amino maleimides **1**–**6**, shown in **Figure 2** would enable us to establish the effects of key substituent choices. Building on previous work on substituent effects of dual hydrogen bond donors, [21] we chose to incorporate aryl rings containing electron-withdrawing and lipophilic trifluoromethyl substituents (-CF_3) at various positions within the scaffold to examine the effect on anion recognition and transport processes. A direct comparison can be drawn between bis-amino maleimides **3** and **4** with **5** and **6**, respectively, where the *N*-methyl group is replaced by an *N*-aryl group. This substitution enables us to probe how the introduction of an electron-withdrawing group (the aromatic ring) can alter the electronics of the maleimide ring and therefore, potentially, adjust its anion binding properties. Analogous unsymmetrical bis-amino maleimides, **1** and **2**, were included in the series to examine the effects of substituting aromatic substituents for aliphatic substituents.

The synthesis of bis-amino maleimides has previously posed a challenge. [48-51] Following amine addition to the dibromomaleimide starting material, the increase in electron density within the maleimide core makes the carbon bearing the bromine substituent less susceptible to nucleophilic attack of a second amine and, as a consequence, symmetrical bis-amino maleimides have so far remained elusive. Here, unsymmetrical bis-amino maleimides, **1** and **2**, were prepared through a facile two-step synthesis from commercially available 2,3-dibromo-*N*-methyl maleimide (**Scheme 1a**). An initial reaction with a poorly nucleophilic aniline (4-(trifluoromethyl)aniline or 3,5-bis(trifluoromethyl)aniline) allowed simple precipitation of the mono-aminated maleimides **7** and **8** from MeOH, avoiding the need for subsequent time-consuming purification steps. A second nucleophilic addition of *n*-butylamine to **7** or **8** in DMF under more forcing conditions formed bis-amino maleimides **1** and **2** in 22% and 34% yield, respectively. While the synthesis of symmetrical bis-amino maleimides remained elusive using this approach, in 2023 Costa and co-workers reported the synthesis of bis-aminated maleic anhydrides (such as **11** and **12**, Scheme 1(b)) via the photochemical ring opening of squaramide precursors. [32] We envisaged that **11** and **12** could be suitable precursors to symmetrical bis-amino maleimides, and correspondingly found that their treatment with either methylamine hydrochloride or an aniline in refluxing AcOH yielded maleimides **3–6**. Working concurrently we also discovered an alternative approach to synthesise bis-amino maleimides starting from intermediates **7** and **8**. By acetylating the first amine substituent, we were able to overcome the problem of maleimide core deactivation thus allowing for nucleophilic addition of a second aniline (see SI section S2.3 for further synthetic details).

Journal Name ARTICLE

View Article Online
DOI: 10.1039/D5OB01392E

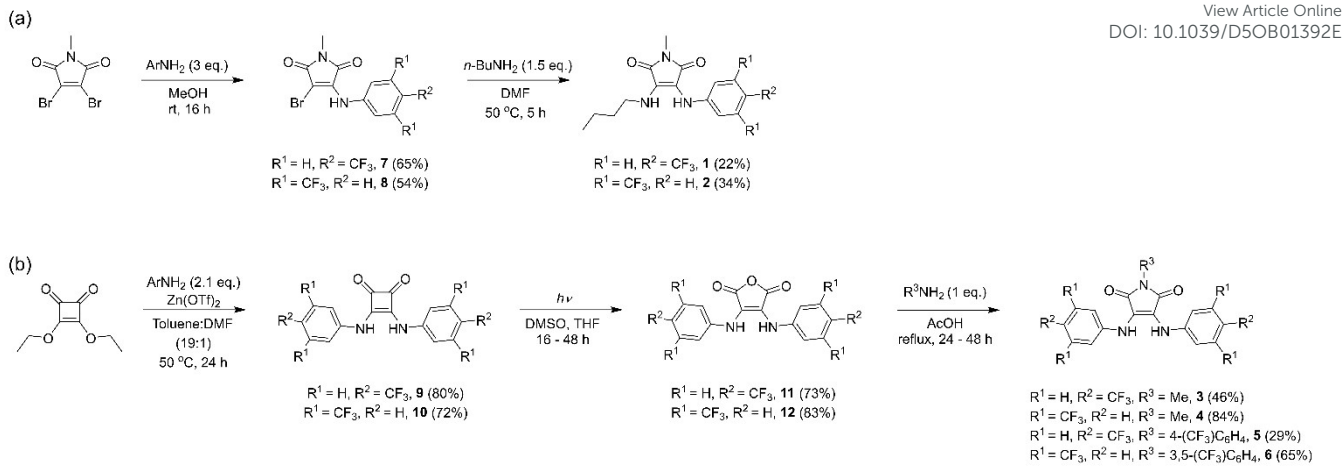

Scheme 1 Synthesis routes to the bis-amino maleimides reported in this work. (**a**) Route to unsymmetrical bis-amino maleimides (**1** and **2**); (**b**) Route to symmetrical bis-amino maleimides (**3**–**6**).

Previous studies have found that mono-amino substituted maleimides can exhibit a range of different fluorescence properties and mechanisms, including twisted intramolecular charge transfer (TICT) and aggregation induced emission (AIE). [48, 49, 52, 53] O'Reilly and co-workers have previously reported that mono-aminated maleimides with aliphatic and benzyl amine substituents exhibit fluorescence properties, [48, 49] although derivatives with aromatic (aniline) substituents, where the maleimide was directly conjugated to the aromatic ring, were found to be non-fluorescent. [49] They suggested that the fluorescence originates from the amino group on the C=C double bond acting as the donor moiety in a donor–acceptor skeleton, with the aryl substituted nitrogen atoms having less electron donating capacity resulting in reduced fluorescence. Other reports suggest that the fluorescence emission properties and mechanism of similar derivatives can be influenced by factors including conformation, intermolecular hydrogen bond formation and the electronic effects of substituents on the maleimide ring. A more in-depth discussion of earlier studies can be found in the SI section S4.3.3.

Interestingly, our symmetrical bis-amino maleimides **3**–**6** bearing two or three aromatic substituents were shown to exhibit weak orange-yellow fluorescence (**Figure 3**), unlike their unsymmetrical counterparts **1** and **2**. In an acetonitrile solution, all of the symmetrical molecules exhibited an emission maximum between 500–600 nm after excitation at 430 nm. The fluorescence emission of **5** displayed a 30 nm red-shift in emission compared to **6**, highlighting the effect of varying the number of electron withdrawing -CF_3 substituents on the aromatic rings. Further analysis of the fluorescence of these molecules in various solvents is shown in the SI section S4. Given the variety of different fluorescence mechanisms exhibited by other amino-substituted maleimides plus the key differences between these literature compounds and our bis-amino maleimides in terms of their conformation (see **Density Functional Theory (DFT) analysis**), intermolecular hydrogen bond formation (see **Anion binding**) and the electronic effects of substituents on the maleimide ring, we do not propose a specific mechanism of fluorescence within our series at present, but further photophysical characterisation may enable this in the future.

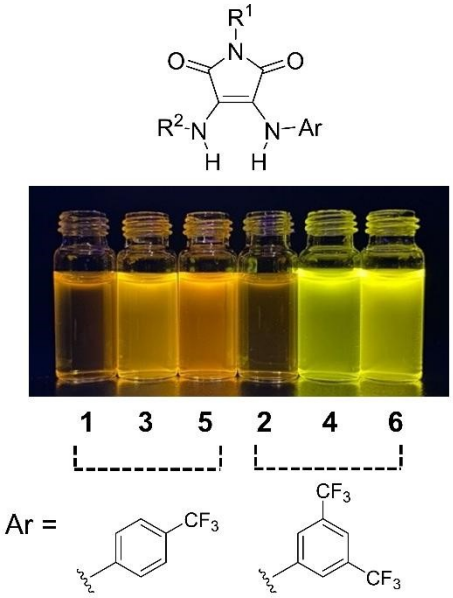

Figure 3 Solutions of **1**–**6** in MeCN emitting fluorescence under UV light (365 nm).

Anion binding

To investigate the halide binding capabilities of **1**–**6**, ^{1}H NMR spectroscopic titration experiments were performed with tetra-*n*-butylammonium chloride, bromide and iodide (TBACl, TBABr and TBAI) in MeCN-d_3 at 298 K. For all of the receptors investigated, the addition of Cl^- caused significant downfield shifts were observed for the N–H maleimide protons (**Figure 4**) which is indicative of hydrogen bond formation and Cl^- binding. In the case of the unsymmetrical receptors **1** and **2**, a smaller overall change in chemical shift was observed for the aliphatic N–H (H_a) compared to the aromatic N–H (H_b), indicating that

this N–H may contribute less to the anion binding. This could be rationalised by considering the relative acidity of the two N–H groups.

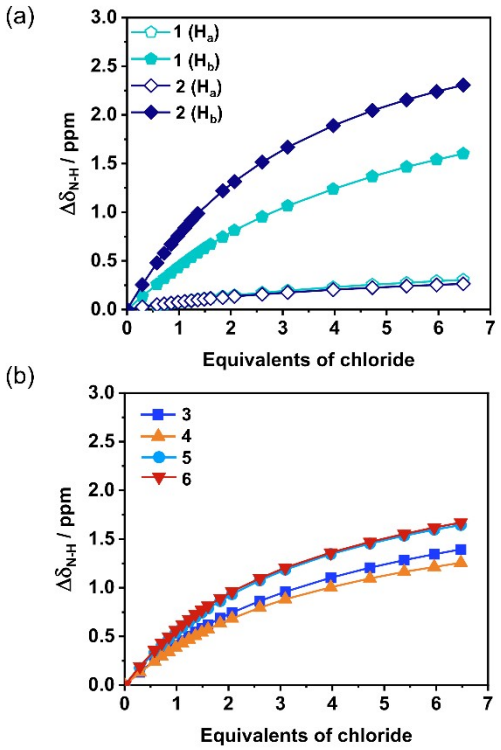

Figure 4 ^{1}H NMR titration studies of symmetrical and unsymmetrical bis-amino maleimides. Plot showing the change in chemical shift of NH protons upon addition of aliquots of TBACl in MeCN-d_3 at 298 K. (**a**) Unsymmetrical bis-amino maleimides (**1–2**); where H_a and H_b represent alkyl and aryl NH protons, respectively); (**b**) Symmetrical bis-amino maleimides (**3–6**).

The Cl^- binding data was analysed using both BindFit[54] and Musketeer, [55] and different binding models were systematically assessed based on the fit quality, random distribution of residuals, errors associated with each fit and root mean squared error (RMSE) analysis as appropriate. [56, 57] Fitting to a 1:1 binding model produced binding constants in the range 22-42 M^{-1} (errors produced by Bindfit < 1% in all cases) with good agreement between Bindfit and Musketeer; however, close inspection of the fitting with both software packages revealed signs that the fit to a 1:1 model was not ideal; in particular the residual analyses showed a sinusoidal distribution, which suggests a systematic error in the fitting. In some cases, close analysis of the normalised fits in Musketeer showed systematic deviation between the experimental data and fitted models. Attempts to fit the Br^- binding data produced binding constants in the range 6–14 M^{-1}, but with similar indications of an imperfect fit to the 1:1 binding model. The titrations with I^- yielded only very small changes in chemical shift, and thus we did not attempt to derive association constants from this data.

Attempts to fit the Cl^- and Br^- titration data to a 1:2 or 2:1 binding model also did not provide satisfactory results, with the residual analyses producing sinusoidal distributions and the RMSE analyses showing less well-defined minima than the 1:1 fitting. This may suggest that a mixture of different binding modes or other equilibria co-exist in solution (SI section S5.3). We conclude, however, that weak Cl^- and Br^- binding is evident across the series. In contrast, squaramide **9** has been previously reported as a strong Cl^- receptor that binds with a 1:1 stoichiometry in both DMSO-d_6/ 0.5% H_2O (K_a = 458 M^{-1} by ^{1}H NMR titration) and MeCN ($K_a = 8.2 \times 10^5$ M^{-1} by UV/ vis titration). [29, 58]

To investigate the binding affinity of **1–6** towards various anions of different sizes and geometries, we also performed ^{1}H NMR spectroscopic titrations with oxoanions (AcO^-, $H_2PO_4^-$, BzO^-), added as their respective TBA salts in MeCN-d_3. Within these titrations, the peak corresponding to the N–H protons initially disappeared, which could be indicative of deprotonation; however other changes in the spectra of unsymmetrical **1** and **2** were observed. In many cases, we observed the emergence of small new peaks in the ^{1}H NMR spectrum when a high equivalence of the more basic anions was added (SI Section S5.4). Maleimides are known to be susceptible to base-mediated hydrolysis which results in opening of the five-membered ring structure, commonly yielding maleamic acids *via* hydrolysis at the imide position. [45, 59] The titration of **1–6** with a strong base (TBAOH) resulted in a complex ^{1}H NMR spectrum which, along with an accompanying colour change from orange to colourless, could signal a breakdown of the core maleimide structure. The isolation and attempted characterisation of one such breakdown product led us to propose the formation of an oxalamide under basic conditions in organic solvents (see SI section S5.7). Given the poor solubility of these derivatives in aqueous solutions, we could not directly monitor their stability in buffers, but we note that aminothiomaleimides are stable to hydrolysis in phosphate buffered saline solutions.[45] We also note that the nucleophilicity of OH^- is likely to be much higher in organic solution (eg. CD_3CN) than in the aqueous buffered conditions relevant to our later transport studies or putative biological applications.

We briefly investigated the application of symmetrical bis-amino maleimides as fluorescent anion sensors but minimal fluorescence quenching was observed upon the addition of TBACl (100 eq.) in MeCN (SI Section S5.8).

Density Functional Theory (DFT) analysis

To better understand the binding properties of the bisaminomaleimides, computational studies were undertaken. For these studies, the butyl groups in **1** and **2** were truncated to methyl groups (giving $\mathbf{1^{Me}}$ and $\mathbf{2^{Me}}$). An initial conformational search was performed for all six maleimides using the Conformer-Rotamer Ensemble Sampling Tool (CREST) developed by Grimme, [62, 63] and the geometries of all conformations identified by CREST were then optimised in ORCA 5.0[64, 65] using the r^{2}SCAN-3c composite method, [66-69] with solvation effects incorporated through the SMD model. [70] For

View Article Online
DOI: 10.1039/D5OB01302F

comparison, the equivalent calculations were also carried out for squaramide **9**, the precursor to **3** and **5** and an established receptor with good affinity for Cl^-.[29, 71]

For the symmetrical bis(arylamino)maleimides **3**–**6**, the conformations located fell into three classes. In each case, the lowest energy conformation was one in which the N-aryl rings were stacked and the N–H bonds pointed away from one another (depicted in **Figure 5a** for **3**). We label this conformation *syn*, *syn* where the *syn* designation refers to the disposition of the N-H bond relative to the adjacent maleimide carbonyl group. The next-lowest energy conformations had an *anti*, *syn* arrangement (**Figure 5b**), with the *anti*, *anti*-conformation (**Figure 5c**), which would be required for chelation to a Cl^- ion, still higher in energy. All *syn* conformations had dihedral angles OC–C–N–H in the range $|\psi| < 25°$, while anti conformations had $|\psi| > 130°$. The alkylamino-substituted unsymmetrical maleimides $\mathbf{1^{Me}}$ and $\mathbf{2^{Me}}$ fell into four conformational classes, with both the arylamino and alkylamino N–H bonds adopting either *syn* or *anti* orientations. For these compounds, the alkylamino N–H bond was always near-coplanar with the maleimide ring, while the arylamino N–H bond was closer to perpendicular to the maleimide than for the bis(arylamino) compounds.

For all of the maleimide ligands **1**–**6**, the *anti*, *anti*-conformation lay between 2.5 kcal/mol and 6.8 kcal/mol higher in free energy than the lowest energy conformation (**Table 1**). By contrast, for squaramide **9** the corresponding difference was only 0.7 kcal/mol (values for all conformers are in the SI Section S6).

Mono-chloride complexes of the six maleimides and of squaramide **9** were also modelled. For every maleimide, it was possible to find both monodentate and bidentate complexes, with the monodentate complex having the lower free energy. The lowest energy mono- and bidentate conformations of **3**–Cl^- are shown in **Figures 5d** and **5e**. For the unsymmetrical maleimides $\mathbf{1^{Me}}$–Cl^- and $\mathbf{2^{Me}}$–Cl^-, the Cl^- was bound to the aryl N–H in the monodentate complexes.

For squaramide **9**, the bidentate complex was markedly lower in energy than the monodentate complex. This bidentate **9**–Cl^- complex was essentially planar (**Figure 5f**), with OC–C–N–H dihedral angles of ±178° (for comparison, the crystal structure of this complex with a tetrabutylammonium cation[29] has dihedral angles of +169.4° and –174.8°) while the bidentate Cl^- complexes of **3**–**6** were twisted away from planarity with dihedral angles in the 140°–160° range. The bidentate complexes of $\mathbf{1^{Me}}$ and $\mathbf{2^{Me}}$ showed the alkyl N–H close to coplanar with the maleimide ring and the aryl N–H at *ca.* 140°

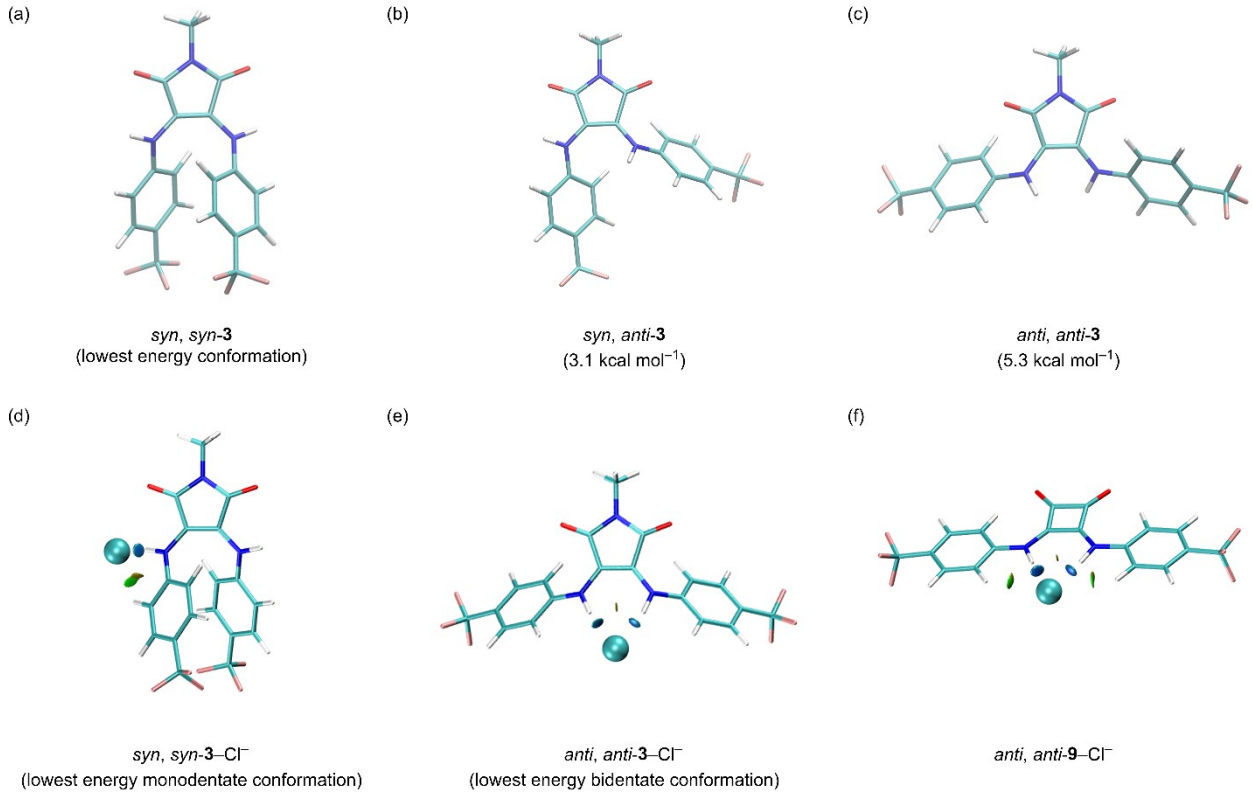

Figure 5 (**a**,**b**,**c**) Three main conformations of receptor **3**. The energy values are Gibbs energies relative to the *syn*, *syn*-conformation; (**d**) Lowest energy conformation of **3**–Cl^-; (**e**) Lowest energy bidentate conformation of **3**–Cl^-; (**f**) Monodentate conformation of **9**–Cl^-. Figures (**d**)–(**f**) also show the isosurface of the reduced density gradient in the vicinity of the Cl^- ion, coloured by sign(λ_2)ρ. Strongly attractive interactions are shown in blue, with weaker attractive interactions in green. This figure was created using the VMD program. [67, 68]

View Article Online
DOI: 10.1039/D5OB01795E

from planarity. Further details of the modelled geometries, including higher energy conformations, are in SI Section 6.

The Cl^- complexes were also subjected to analysis using the QTAIM (Quantum Theory of Atoms in Molecules) method. [74-76] Bond critical points were located for all the expected NH–Cl interactions; in each case a positive value of $\nabla^2\rho$ was found, consistent with a hydrogen-bonding interaction. For each of the monodentate maleimide complexes, a further CH–Cl bond critical point was found, involving the methyl group of **1^{Me}** and **2^{Me}**, and an *ortho*-CH of the bis(arylamino) compounds. **Figures 5d** and **5e** show the monodentate and bidentate **3**–Cl^- complexes with the isosurface of the reduced density gradient[77] coloured according to $\mathrm{sign}(\lambda_2)\rho$ – the stronger NH–Cl interaction is shown in blue, with the weaker CH–Cl interaction in green. [75, 76] The bidentate squaramide complex **9**–Cl^- displayed two such CH–Cl interactions (**Figure 5f**), but none were found in the bidentate maleimide complexes. C-H hydrogen bonds have previously been suggested to play a role in binding of trifluoromethylated arylamino groups to Lewis basic substrates. [78] Hydrogen bond strengths E_{HB} were also calculated from the potential energy density at the critical point of each H–Cl bond; [79] these, together with the calculated free energies of binding in kcal mol^{-1} for the monodentate and bidentate Cl^- complexes and the energy differences between the *syn*,*syn*- and *anti, anti*-conformations of the ligands, are shown in **Table 1**.

The data in **Table 1** suggest that the binding of the maleimide receptors to Cl^- is markedly weaker than that of squaramide **9**, and that all of the maleimides have similar binding affinities, which is in line with our experimental binding analysis. Furthermore, a monodentate binding mode was found to be most favourable for the maleimide receptors, in contrast to the squaramide.

A large portion of the difference between the binding of the maleimides and the squaramide can be accounted for by the stronger preference of the maleimides for the *syn*,*syn*-conformation; in addition, the NH–Cl hydrogen bonds formed in bidentate **9**–Cl^- are stronger, and there are also contributions from two CH–Cl hydrogen bonds.

The favourable nature of monodentate chloride binding for the maleimide receptors also opens the possibility that these ligands could bind to two chloride ions, one for each N–H, although this was not explored computationally. The presence of multiple potential, low energy binding modes and conformations for the maleimide receptors could explain the imperfect fit to simple binding models observed in our attempts to fit our experimental titration data, particularly the difficulty in assigning the binding stoichiometry.

Table 1 Calculated binding data for model receptors **1^{Me}** and **2^{Me}**, receptors **3–6**, and squaramide **9**. All calculations were at the r^{2}SCAN-3c/SMD(MeCN) level.

Receptor[a]		ΔG_{bind} / kcal mol^{-1}	ΔG_{conf} / kcal mol^{-1} [b]	E_{HB} (NH-Cl)/ kcal mol^{-1} [c]	E_{HB} (CH-Cl)/ kcal mol^{-1} [c]
1^{Me}	mono[d]	–0.4		–9.5	–3.8
	bi	–0.1	2.7	–8.6, –8.2	[e]
2^{Me}	mono[d]	–1.8		–10.2	–3.8
	bi	–0.9	2.5	–8.8, –8.1	[e]
3	mono	–0.4		–9.8	–3.6
	bi	0.8	5.3	–9.6, –9.5	[e]
4	mono	–0.4		–9.8	–4.4
	bi	1.4	6.8	–9.0, –8.4	[e]
5	mono	–1.1		–10.1	–3.8
	bi	–0.2	3.7	–9.8, –9.7	[e]
6	mono	–1.9		–10.1	–3.7
	bi	0.3	5.9	–10.3, –9.9	[e]
9	mono	–1.3		–10.9	–3.6
	bi	–5.6	0.7	–10.2, –10.2	–3.1, –3.1

[a] mono and bi refer to the monodentate and bidentate mono-chloride complexes. [b] Free energy difference between the lowest-energy *syn, syn* and *anti, anti* conformations of the unbound receptor. [c] Hydrogen bond strengths calculated from the potential energy density at the bond critical point. [79] [d] The Cl^- ion is coordinated to the aryl N–H. [e] No CH–Cl bond critical points were identified.

Anion transport activity

The anion transport activity of **1**–**6** was initially investigated using a Cl^-/NO_3^- transmembrane exchange assay using a Cl^- ion selective electrode (ISE) (depicted in **Figure 6a**). Unilamellar 1-palmitoyl-2-oleoyl-sn-glycero-3-phosphocholine (POPC) vesicles were prepared containing NaCl buffered to pH 7.2. The vesicles were suspended in $NaNO_3$ (pH 7.2). Addition of the transporter as a DMSO solution (10 mol% transporter to lipid) initiated the experiment, and the resulting Cl^- efflux was monitored using an ISE. At the end of the experiment, detergent was added to lyse the vesicles for calibration of 100% Cl^- release. The results are shown in **Figure 6b**. These studies found that **5** was the only bis-amino maleimide to display any anionophoric potential. By comparison, the other five bis-amino

Journal Name ARTICLE

View Article Online
DOI: 10.1039/D5OB01393E

maleimides all showed minimal Cl^- transport (<10% efflux; **Figure 6b**, **Table 2**).

When designing a successful anion transporter, lipophilicity is highly significant. Previous studies have shown that there is a fine balance between a molecule being highly lipophilic to partition readily into the lipid bilayer and being sufficiently soluble in the aqueous phase to enable delivery to the membrane. [80-82] As the shape of our transport activity curve for **5** was sigmoidal after transporter addition (indicating a lag phase before effective transport was observed), we sought to further investigate whether the poor deliverability of bis-amino maleimides **1**–**6** could be inhibiting the transport process. We found that addition of **5** and **6** from a more dilute DMSO solution yielded increased Cl^- efflux (SI section S7.3), which could indicate that the delivery of the transporter to the membrane is improved by the larger quantity of DMSO and is thus a limiting factor. The other derivatives **1**–**4** remained inactive under these conditions (SI section S7.3). The key structural difference between **5** and **6** vs the other derivatives is that they contain an electron poor aryl substituent in the imide position (*vs* a methyl group); this demonstrates the significant potential in fine-tuning the anion transport function of this class of molecules based on our new functional handle. The anion transport activity of **5** in the Cl^-/NO_3^- antiport assay was quantified by Hill analysis, allowing the EC_{50} value, defined as the concentration of transporter (mol% transporter to lipid) required to obtain 50% efflux at 270 s, to be calculated as 4.1 mol% w.r.t. lipid. By comparison, squaramide **9** is a more potent anionophore (EC_{50} 0.06 mol%),[29] although it can be challenging to deliver due to solubility issues. [83]

We carried out further mechanistic studies into the anion transport action of **5**. Firstly, we conducted a Cl^-/HCO_3^- antiport assay using a Cl^- ISE (SI section S7.5). The results demonstrated that **5** is capable of mediating low levels of Cl^-/ HCO_3^- exchange (EC_{50} = 10.1 mol% w.r.t. lipid), and also confirmed that no transport is observed in the absence of an external anion that can be readily transported – this implying that **5** functions as an anion antiporter. We then conducted a cationophore-coupled transport assay (depicted in **Figure 6 c-d**), used to investigate if an anionophore is capable of functioning by an electrogenic or

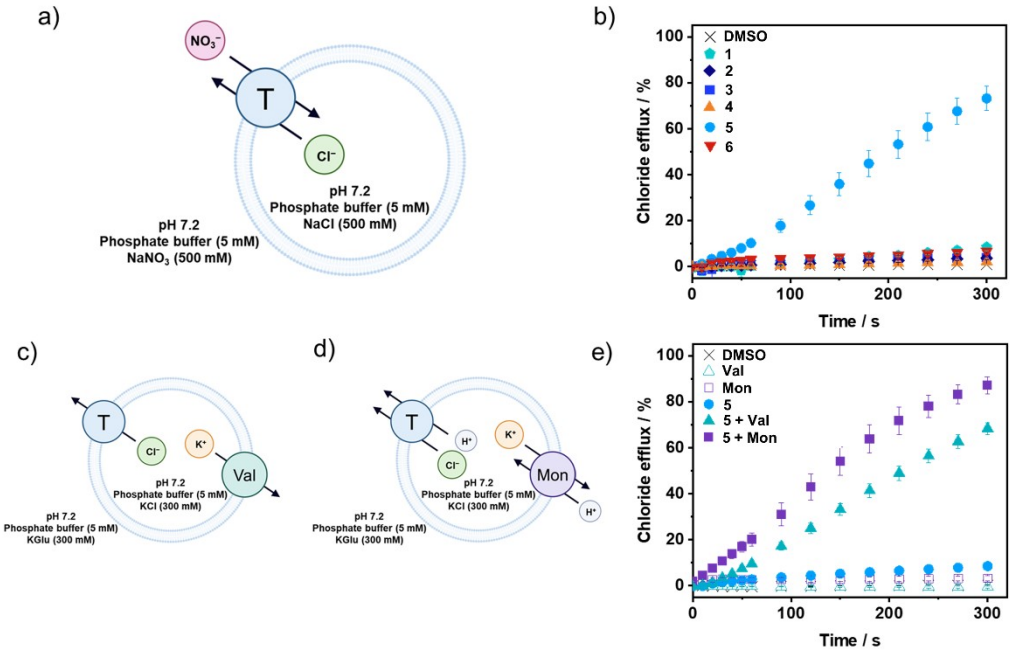

Figure 6 (**a**) A schematic representation of the Cl^-/NO_3^- antiport assay; (**b**) Cl^- efflux facilitated by receptors **1**–**6** (10 mol% transporter to lipid) in the Cl^-/NO_3^- antiport assay; (**c-d**) a schematic representation of the cationophore-coupled transport assay with valinomycin and monensin; (**e**) Cl^- efflux (%) facilitated by **5** (5 mol% transporter to lipid) only and in the presence of valinomycin (Val, 0.1 mol%) and monensin (Mon, 0.1 mol%) in the cationophore-coupled transport assay. At the end of each transport assay, the vesicles were lysed with detergent to calibrate 100% efflux. Error bars represent the standard deviation of three experiments.

electroneutral transport processes. [84] In this assay, the efflux of Cl^- from KCl containing vesicles suspended in KGlu (where Glu = gluconate, a hydrophilic anionic species assumed not to be transported under these experimental conditions) is monitored using a Cl^- ISE. The transport efficiency in the presence and absence of two different cationophores – valinomycin and monensin – is compared. Enhanced transport in the presence of valinomycin (a potassium uniporter) implies that the transporter is capable of electrogenic transport (a transport process that would lead to a build-up of charge), while enhanced transport in the presence of monensin (a K^+/H^+ antiporter) implies that the transport is capable of electroneutral transport (an overall charge neutral transport process such as H^+/Cl^- co-transport).

View Article Online
DOI: 10.1039/D5OB01392E

Table 2 Summary of the anion transport properties of bis-amino maleimides, **1**-**6**, including calculated LogP values.

Transporter	Cl^- efflux[a] (%)	LogP[b]	$EC_{50,\ 270s}$[c] (mol%)	n[d]
1	7.0	2.0	-[e]	-[e]
2	3.4	2.9	-[e]	-[e]
3	3.6	3.2	-[e]	-[e]
4	1.9	4.9	-[e]	-[e]
5	67.2	5.7	4.12[f]	3.13[f]
6	6.2	8.3	-[e]	-[e]

[a] Maximum Cl^- efflux values taken at 270 s after transporter addition (10 mol% transporter to lipid). [b] Predicted LogP values obtained from ChemAxon lipophilicity calculator. [c] $EC_{50,\ 270s}$ defined as the concentration of transporter (mol% transporter to lipid) required to obtain 50% Cl^- efflux at 270 s. [d] *n* defined as Hill coefficient. [e] Hill analysis could not be performed due to low transport activity. [f] Values for $EC_{50,\ 270s}$ and *n* determined from Hill analysis using a 1.25 mM stock solution.

Our results, shown in **Figure 6e**, show a significant acceleration in the rate of Cl^- efflux facilitated by **5** when in the presence of both valinomycin and monensin compared to **5** alone, indicating that **5** is capable of both electrogenic and electroneutral Cl^- transport. Finally, we conducted a preliminary investigation into the selectivity of **5** for transporting Cl^- vs H^+ or OH^- using a fluorescence assay involving 8-hydroxypyrene-1,3,6-trisulfonic acid (HPTS), [85] a ratiometric, pH responsive fluorescent probe coupled with the proton channel gramicidin (SI section S7.7). Vesicles were prepared containing HPTS in NMDG-Cl buffered to pH 7 (where NMDG = *N*-methyl-D-glucamine, a monovalent and highly hydrophilic cation assumed not to be transported under these experimental conditions). The external solution contained NMDG-Cl buffered to pH 7, and after the addition of the transporter(s), the experiment was initiated by adding a base pulse to create a pH gradient. Subsequent changes in the ratiometric HPTS fluorescence was indicative of an increase in the pH inside the vesicles. The results showed that **5** is able to dissipate the pH gradient both in the absence and presence of gramicidin, and that the rate of transport is slightly elevated in the presence of gramicidin. This further implies that **5** is capable of both electroneutral (H^+/Cl^- symport or Cl^-/OH^- antiport) and electrogenic Cl^- transport, potentially with some selectivity for electrogenic transport.

Conclusions

In this study we have demonstrated the successful synthesis of a series of symmetrical and unsymmetrical bis-amino maleimides that are able to function as anion receptors for Cl^-. Weak Cl^- binding in MeCN-d_3 was observed via ^{1}H NMR titration, and imperfect fits to simple binding models may imply that multiple binding modes or equilibria exist in solution. DFT analysis indicated that multiple conformations of these receptors exist, meaning that (i) the receptors need to re-organise from their lowest energy conformation in order to form a bidentate cleft for anions, and (ii) monodentate binding may also be possible. These findings could explain the apparently weak anion affinity and difficulties in fitting the titration data to simple binding models. This trend is similar to that displayed by other five-membered dual hydrogen bond donors and demonstrates the limitations of using this rigid (N-containing) five membered ring structure in a receptor, as a conformational change is required to bind an anion in a 1:1 binding mode. The anion transport activity of bis-amino maleimides was investigated using the Cl^-/NO_3^- antiport assay and receptor **5** (and to a limited degree, **6**) were found to display anionophoric activity, with Hill analysis showing a EC_{50} value of 4.1 mol% w.r.t lipid for receptor **5**. This finding demonstrates that substitution at the imide nitrogen can tune the function of this class of receptors. Overall this work has established the utility of the bis-amino maleimide scaffold in anion recognition and transport, and demonstrated key design principles that can influence binding strength, pre-organisation and transport activity. By comparison to squaramides, which are established anion receptors and transporters, our bis-amino maleimides show lower activities at present but offer more opportunities for synthetic diversification.

Author contributions

The authors of this manuscript contributed to the project as follows: **Evelyn R. Morton**: conceptualisation; data curation; formal analysis; investigation; methodology; visualisation; writing – original draft preparation; writing – review and editing. **Michael J. Porter**: data curation, formal analysis, investigation, methodology, resources, supervision, visualisation, writing – original draft preparation; writing – review and editing. **James R. Baker**: conceptualisation, methodology, project administration, resources, supervision, writing – review and editing. **Vijay Chudasama**: conceptualisation, methodology, project administration, resources, supervision, writing – review and editing. **Cally J. E. Haynes**: conceptualisation; formal analysis; funding acquisition; investigation; methodology; project administration; resources; supervision; visualisation; writing – original draft preparation; writing – review and editing.

Conflicts of interest

There are no conflicts to declare.

Data availability

The data supporting this article have been included as part of the Supplementary Information.

Acknowledgements

The authors thank Roopender Kumar for advice and guidance on photochemical reactions, and Daniil Soloviev and Larissa von Krbek for helpful discussions about the binding analysis. CJEH and ERM gratefully acknowledge UCL Chemistry for a PhD studentship and EPSRC (EP/T025735/1).

Notes and references

1. L. K. Macreadie, A. M. Gilchrist, D. A. McNaughton, W. G. Ryder, M. Fares and P. A. Gale, *Chem*, 2022, **8**, 46-118.
2. G. T. Williams, C. J. E. Haynes, M. Fares, C. Caltagirone, J. R. Hiscock and P. A. Gale, *Chem. Soc. Rev.*, 2021, **50**, 2737-2763.
3. D. A. McNaughton, W. G. Ryder, A. M. Gilchrist, P. Wang, M. Fares, X. Wu and P. A. Gale, *Chem*, 2023, **9**, 3045-3112.
4. K. Maslowska-Jarzyna, E. York, E. Feo, R. M. Maklad, G. Bao, M. Fares and P. A. Gale, *Chem*, 2025, DOI: 10.1016/j.chempr.2025.102695.
5. M. Gentzsch and M. A. Mall, *Chest*, 2018, **154**, 383-393.
6. E. Feo and P. A. Gale, *Curr. Opin. Chem. Biol.*, 2024, **83**, 102535.
7. L. E. Brennan, X. Luo, F. A. Mohammed, K. Kavanagh and R. B. P. Elmes, *Chem. Sci.*, 2025, DOI: 10.1039/D4SC01693A.
8. L. E. Brennan, L. K. Kumawat, M. E. Piatek, A. J. Kinross, D. A. McNaughton, L. Marchetti, C. Geraghty, C. Wynne, H. Tong, O. N. Kavanagh, F. O'Sullivan, C. S. Hawes, P. A. Gale, K. Kavanagh and R. B. P. Elmes, *Chem*, 2023, **9**, 3138-3158.
9. H. Li, H. Valkenier, A. G. Thorne, C. M. Dias, J. A. Cooper, M. Kieffer, N. Busschaert, P. A. Gale, D. N. Sheppard and A. P. Davis, *Chem. Sci.*, 2019, **10**, 9663-9672.
10. J. Torrisi, M. Chvojka, P. Jurček, X. Zhang, H. Zeng, V. Šindelář and H. Valkenier, *Angew. Chem. Int. Ed.*, 2025, **64**, e202424754.
11. S. B. Salunke, S. N. Save, N. J. Roy, R. Naorem, S. Sharma and P. Talukdar, *Org. Biomol. Chem.*, 2024, **22**, 4987-4992.
12. J. Yang, G. Yu, J. L. Sessler, I. Shin, P. A. Gale and F. Huang, *Chem*, 2021, **7**, 3256-3291.
13. S. Das, R. Karn, M. Kumar, S. Srimayee and D. Manna, *Org. Biomol. Chem.*, 2024, **22**, 114-119.
14. M. K. Kar, R. Mahata, S. Srimayee, N. Haloi, R. Kumar, E. Lindahl, M. K. Santra and D. Manna, *Chem. Commun.*, 2024, **60**, 8419-8422.
15. G. Picci, I. Carreira-Barral, D. Alonso-Carrillo, C. Busonera, J. Milia, R. Quesada and C. Caltagirone, *Org. Biomol. Chem.*, 2022, **20**, 7981-7986.
16. A. Arias-Betancur, P. Fontova, D. Alonso-Carrillo, I. Carreira-Barral, J. Duis, M. García-Valverde, V. Soto-Cerrato, R. Quesada and R. Pérez-Tomás, *Biochem Pharmacol*, 2024, **229**, 116469. DOI: 10.1039/D5OB01392E
17. M. Pérez-Hernández, C. Cuscó, C. Benítez-García, J. Bonelli, M. Nuevo-Fonoll, A. Soriano, D. Martínez-García, A. Arias-Betancur, M. García-Valverde, M. F. Segura, R. Quesada, J. Rocas, V. Soto-Cerrato and R. Pérez-Tomás, *Biomedicines*, 2021, **9**, 508.
18. M. Fares, X. Wu, D. A. McNaughton, A. M. Gilchrist, W. Lewis, P. A. Keller, A. Arias-Betancur, P. Fontova, R. Pérez-Tomás and P. A. Gale, *Org. Biomol. Chem.*, 2023, **21**, 2509-2515.
19. A. Mondal, M. Siwach, M. Ahmad, S. K. Radhakrishnan and P. Talukdar, *ACS Infect. Dis.*, 2024, **10**, 371-376.
20. N. Busschaert, I. L. Kirby, S. Young, S. J. Coles, P. N. Horton, M. E. Light and P. A. Gale, *Angew. Chem. Int. Ed.*, 2012, **51**, 4426-4430.
21. N. Busschaert, M. Wenzel, M. E. Light, P. Iglesias-Hernández, R. Pérez-Tomás and P. A. Gale, *J. Am. Chem. Soc.*, 2011, **133**, 14136-14148.
22. N. J. Andrews, C. J. E. Haynes, M. E. Light, S. J. Moore, C. C. Tong, J. T. Davis, W. A. Harrell Jr and P. A. Gale, *Chem. Sci.*, 2011, **2**, 256-260.
23. B. A. McNally, A. V. Koulov, T. N. Lambert, B. D. Smith, J. B. Joos, A. L. Sisson, J. P. Clare, V. Sgarlata, L. W. Judd, G. Magro and A. P. Davis, *Chem.Eur. J.*, 2008, **14**, 9599-9606.
24. V. Amendola, L. Fabbrizzi and L. Mosca, *Chem. Soc. Rev.*, 2010, **39**, 3889-3915.
25. J. Gomez-Vega, A. Vasquez-Cornejo, O. Juárez-Sánchez, D. O. Corona-Martínez, A. Ochoa-Terán, K. A. López-Gastelum, R. R. Sotelo-Mundo, H. Santacruz-Ortega, J. C. Gálvez-Ruiz, R. Pérez-González and K. O. Lara, *ACS Omega*, 2024, **9**, 4412-4422.
26. L. Qin, A. Hartley, P. Turner, R. B. P. Elmes and K. A. Jolliffe, *Chem. Sci.*, 2016, **7**, 4563-4572.
27. C. Jin, M. Zhang, L. Wu, Y. Guan, Y. Pan, J. Jiang, C. Lin and L. Wang, *Chem. Commun.*, 2013, **49**, 2025-2027.
28. G. Picci, R. Montis, V. Lippolis and C. Caltagirone, *Chem. Soc. Rev.*, 2024, **53**, 3952-3975.
29. N. Busschaert, I. L. Kirby, S. Young, S. J. Coles, P. N. Horton, M. E. Light and P. A. Gale, *Angew. Chem. Int. Ed.*, 2012, **51**, 4426-4430.
30. A. Jeppesen, B. E. Nielsen, D. Larsen, O. M. Akselsen, T. I. Sølling, T. Brock-Nannestad and M. Pittelkow, *Org. Biomol. Chem.*, 2017, **15**, 2784-2790.
31. V. E. Zwicker, K. K. Y. Yuen, D. G. Smith, J. Ho, L. Qin, P. Turner and K. A. Jolliffe, *Chem. Eur. J.*, 2018, **24**, 1140-1150.
32. M. Vega, L. Martínez-Crespo, M. Barceló-Oliver, C. Rotger and A. Costa, *Org. Lett.*, 2023, **25**, 3423-3428.
33. N. Busschaert, S. J. Bradberry, M. Wenzel, C. J. E. Haynes, J. R. Hiscock, I. L. Kirby, L. E. Karagiannidis, S. J. Moore, N. J. Wells, J. Herniman, G. J. Langley, P. N. Horton, M. E. Light, I. Marques, P. J. Costa, V. Félix, J. G. Frey and P. A. Gale, *Chem. Sci.*, 2013, **4**, 3036-3045.
34. L. E. Bickerton and M. J. Langton, *Chem. Sci.*, 2022, **13**, 9531-9536.
35. D. A. McNaughton, M. Fares, G. Picci, P. A. Gale and C. Caltagirone, *Coord. Chem. Rev.*, 2021, **427**, 213573.
36. W. G. Ryder, A. Levina, M. E. Graziotto, B. A. Hawkins, D. E. Hibbs, E. J. New and P. A. Gale, *Chem*, 2025, **11**.
37. P. Peluso and B. Chankvetadze, *Chem. Rev.*, 2022, **122**, 13235-13400.

38. A. Kerckhoffs and M. J. Langton, *Chem. Sci.*, 2020, **11**, 6325-6331.
39. M. Konopka, L. Halgreen, A.-E. Dascalu, M. Chvojka and H. Valkenier, *Chem. Sci.*, 2025, DOI: 10.1039/D4SC08580A.
40. S. Chattopadhayay, P. Wanjari and P. Talukdar, *Chem. Sci.*, 2024, **15**, 17017-17025.
41. S. J. Wezenberg, L.-J. Chen, J. E. Bos, B. L. Feringa, E. N. W. Howe, X. Wu, M. A. Siegler and P. A. Gale, *J. Am. Chem. Soc.*, 2022, **144**, 331-338.
42. A. Kerckhoffs, M. Ahmad and M. J. Langton, *Chem. Eur. J.*, 2024, **30**, e202402382.
43. S. Byrne and K. M. Mullen, *Supramol. Chem.*, 2018, **30**, 196-205.
44. B. Zavala-Contreras, H. Santacruz-Ortega, A. U. Orozco-Valencia, M. Inoue, K. Ochoa Lara and R.-E. Navarro, *ACS Omega*, 2021, **6**, 9381-9390.
45. A. Wall, A. G. Wills, N. Forte, C. Bahou, L. Bonin, K. Nicholls, M. T. Ma, V. Chudasama and J. R. Baker, *Chem. Sci.*, 2020, **11**, 11455-11460.
46. N. Forte, V. Chudasama and J. R. Baker, *Drug Discov. Today Technol.*, 2018, **30**, 11-20.
47. L. Castañeda, Z. V. F. Wright, C. Marculescu, T. M. Tran, V. Chudasama, A. Maruani, E. A. Hull, J. P. M. Nunes, R. J. Fitzmaurice, M. E. B. Smith, L. H. Jones, S. Caddick and J. R. Baker, *Tetrahedron Lett.*, 2013, **54**, 3493-3495.
48. Y. Xie, J. T. Husband, M. Torrent-Sucarrat, H. Yang, W. Liu and R. K. O'Reilly, *Chem. Commun.*, 2018, **54**, 3339-3342.
49. A. B. Mabire, M. P. Robin, W.-D. Quan, H. Willcock, V. G. Stavros and R. K. O'Reilly, *Chem. Commun.*, 2015, **51**, 9733-9736.
50. E. Awuah and A. Capretta, *J. Org. Chem.*, 2011, **76**, 3122-3130.
51. J. M. J. M. Ravasco, H. Faustino, A. Trindade and P. M. P. Gois, *Chem. Eur. J.*, 2019, **25**, 43-59.
52. T. Kato and K. Naka, *Chem. Lett.*, 2012, **41**, 1445-1447.
53. M. Boominathan, V. Sathish, M. Nagaraj, N. Bhuvanesh, S. Muthusubramanian and S. Rajagopal, *RSC Adv.*, 2013, **3**, 22246-22252.
54. Bindfit, www.supramolecular.org.
55. D. O. Soloviev and C. A. Hunter, *Chem. Sci.*, 2024, **15**, 15299-15310.
56. P. Thordarson, *Chem. Soc. Rev.*, 2011, **40**, 1305-1323.
57. D. Brynn Hibbert and P. Thordarson, *Chem. Commun.*, 2016, **52**, 12792-12805.
58. Y. Yang, X. Wu, N. Busschaert, H. Furuta and P. A. Gale, *Chem. Commun.*, 2017, **53**, 9230-9233.
59. M. E. B. Smith, M. B. Caspersen, E. Robinson, M. Morais, A. Maruani, J. P. M. Nunes, K. Nicholls, M. J. Saxton, S. Caddick, J. R. Baker and V. Chudasama, *Org. Biomol. Chem.*, 2015, **13**, 7946-7949.
60. M. Machida, M. I. Machida and Y. Kanaoka, *Chem. Pharm. Bull.*, 1977, **25**, 2739-2743.
61. C. P. Ryan, M. E. B. Smith, F. F. Schumacher, D. Grohmann, D. Papaioannou, G. Waksman, F. Werner, J. R. Baker and S. Caddick, *Chem. Commun.*, 2011, **47**, 5452-5454.
62. P. Pracht, F. Bohle and S. Grimme, *Phys. Chem. Chem. Phys.*, 2020, **22**, 7169-7192.
63. S. Grimme, *J. Chem. Theory Comput.*, 2019, **15**, 2847-2862.
64. F. Neese, *WIREs Comput. Mol. Sci.*, 2012, **2**, 73-78.
65. F. Neese, *WIREs Comput. Mol. Sci.*, 2022, **12**, e1606.
66. S. Grimme, A. Hansen, S. Ehlert and J.-M. Mewes, *J. Chem. Phys.*, 2021, **154**.
67. H. Kruse and S. Grimme, *J. Chem. Phys.*, 2012, **136**.
68. E. Caldeweyher, C. Bannwarth and S. Grimme, *J. Chem. Phys.*, 2017, **147**.
69. E. Caldeweyher, S. Ehlert, A. Hansen, H. Neugebauer, S. Spicher, C. Bannwarth and S. Grimme, *J. Chem. Phys.*, 2019, **150**.
70. A. V. Marenich, C. J. Cramer and D. G. Truhlar, *J. Phys. Chem. B*, 2009, **113**, 6378-6396.
71. V. Amendola, L. Fabbrizzi, L. Mosca and F.-P. Schmidtchen, *Chem. Eur. J.*, 2011, **17**, 5972-5981.
72. VMD program, http://www.ks.uiuc.edu/Research/vmd/.
73. W. Humphrey, A. Dalke and K. Schulten, *J. Mol. Graph.*, 1996, **14**, 33-38.
74. R. F. W. Bader, *Chem. Rev.*, 1991, **91**, 893-928.
75. QTAIM analysis and calculation of reduced density gradients were carried out using MultiWFN 3.8., T. Lu, *J. Chem. Phys.*, 2024, **161**, 082503.
76. T. Lu and F. Chen, *J. Comput. Chem.*, 2012, **33**, 580-592.
77. E. R. Johnson, S. Keinan, P. Mori-Sánchez, J. Contreras-García, A. J. Cohen and W. Yang, *J. Am. Chem. Soc.*, 2010, **132**, 6498-6506.
78. K. M. Lippert, K. Hof, D. Gerbig, D. Ley, H. Hausmann, S. Guenther and P. R. Schreiner, *Eur. J. Org. Chem.*, 2012, **2012**, 5919-5927.
79. E. Espinosa, E. Molins and C. Lecomte, *Chem. Phys. Lett.*, 1998, **285**, 170-173.
80. C. J. E. Haynes, N. Busschaert, I. L. Kirby, J. Herniman, M. E. Light, N. J. Wells, I. Marques, V. Felix and P. A. Gale, *Org. Biomol. Chem.*, 2014, **12**, 62-72.
81. V. Saggiomo, S. Otto, I. Marques, V. Félix, T. Torroba and R. Quesada, *Chem. Commun.*, 2012, **48**, 5274-5276.
82. C. J. E. Haynes, S. J. Moore, J. R. Hiscock, I. Marques, P. J. Costa, V. Felix and P. A. Gale, *Chem. Sci.*, 2012, **3**, 1436-1444.
83. K. Yang, L. C. Lee, H. A. Kotak, E. R. Morton, S. M. Chee, D. P. M. Nguyen, A. Keskküla and C. J. E. Haynes, *Chem. Methods*, 2025, **n/a**, e202400084.
84. N. Busschaert, S.-H. Park, K.-H. Baek, Y. P. Choi, J. Park, E. N. W. Howe, J. R. Hiscock, L. E. Karagiannidis, I. Marques, V. Félix, W. Namkung, J. L. Sessler, P. A. Gale and I. Shin, *Nat. Chem.*, 2017, **9**, 667-675.
85. A. M. Gilchrist, W. Patrick, C.-B. Israel, A.-C. Daniel, W. Xin, Q. Roberto and P. A. and Gale, *Supramol. Chem.*, 2021, **33**, 325-344.

View Article Online
DOI: 10.1039/D5OB01392E

The data supporting this article have been included as part of the Supplementary Information.